Reed, G. H., Barlow, C. H., & Burns, R. A., Jr. (1978) *J. Biol. Chem. 253*, 4153.
Rose, I. A., O'Connell, E. L., Litwin, S., & Bar-Tana, J. (1974) *J. Biol. Chem. 249*, 5163.
Rowley, G. L., Greenleaf, A. L., & Kenyon, G. L. (1971) *J. Am. Chem. Soc. 93*, 5542.
Schimerlik, M. I., & Cleland, W. W. (1973) *J. Biol. Chem. 248*, 8418.
Schmidt, D. E., Jr., & Westheimer, F. H. (1971) *Biochemistry 10*, 1249.
Smith, D. J., & Kenyon, G. L. (1974) *J. Biol. Chem. 249*, 3317.
Steitz, T. A., Anderson, W. F., Fletterick, R. J., & Anderson, C. M. (1977) *J. Biol. Chem. 252*, 4494.
Viola, R. E., & Cleland, W. W. (1978) *Biochemistry 17*, 4111.
Watts, D. C., & Rabin, B. R. (1962) *Biochem. J. 85*, 507.

Interactions between Apoaspartate Aminotransferase and Pyridoxal 5′-Phosphate. A Stopped-Flow Study†

D. Vergé* and M. Arrio-Dupont

ABSTRACT: The fast kinetics and mechanism of the reconstitution reaction of holoaspartate aminotransferase from apoenzyme and pyridoxal 5′-phosphate were investigated by the stopped-flow method. When the absorbance change was monitored at 362 nm, the process was shown to involve three steps. The dependence of the three relaxation times on pyridoxal 5′-phosphate concentration and the analysis of the amplitudes enabled us to propose a mechanism in which the initial reversible binding step was followed by two irreversible isomerization steps. The rate constants and the extinction coefficients at 362 nm of the intermediate species were determined. Studies of the reconstitution under the stoichiometric conditions at various wavelengths confirmed the occurrence of at least three steps, and especially of the last decoupled step, but strongly suggest that the actual mechanism is more complex.

During the formation of the active structure of an enzyme, it is interesting to study the last steps of the process to understand the formation of a catalytic structure. Stable structures are encountered for which no activity can be observed and for which some conformational changes are necessary to obtain the catalytic form. The best examples of these phenomena are the activation of zymogens to give active enzymes by proteolytic cleavage and the interaction of coenzymes with apoenzymes to give active holoenzymes. Pyridoxal phosphate enzymes are especially suitable for this kind of study because spectroscopic characteristics of free and bound coenzyme are very different and allow the easy observation of the binding of the coenzyme.

We chose to study aspartate aminotransferase,[1] for which the binding of pyridoxal phosphate is quasi-irreversible and for which important differences have been observed [cf. the review by Braunstein (1973)] between free and bound coenzyme. In this enzyme, conformational changes between apo- and holoenzyme are evidenced from experiments based upon stability toward urea denaturation (Ivanov et al., 1973), fluorescence of aromatic residues (Arrio-Dupont, 1978), and hydrogen–deuterium exchange (Abaturov et al., 1968). It has been shown that the kinetics of reconstitution of the apoenzyme are very dependent on the mode of preparation of the apoenzyme (Arrio-Dupont, 1972). An apoenzyme prepared in the presence of phosphate according to Scardi (1963) is slowly reactivated. After phosphate removal by precipitation with $(NH_4)_2SO_4$ (Furbish et al., 1969), the rate of reconstitution is increased, and it has been shown by Fonda & Auerbach (1976) that the kinetics follow a two-step process. The rate of reconstitution of an apoenzyme prepared according to Wada & Snell (1962), i.e., without phosphate, is faster than that of the apoenzyme prepared according to Furbish et al. (1969) (Arrio-Dupont, 1972). In this paper, the binding process of pyridoxal phosphate to apoenzyme prepared without inorganic phosphate is studied and some spectroscopic characteristics of the intermediary species are described.

Experimental Procedures

Materials

Enzymes. The α form of holoaspartate aminotransferase was prepared from pig heart cytosol according to Martinez-Carrion et al. (1967). Apoenzyme free of inorganic phosphate was obtained as previously described by a method adapted from Wada & Snell (1962) (Arrio-Dupont, 1972). Protein concentrations were calculated from spectrophotometric measurements using $\epsilon_{280} = 1.32\ 10^5\ M^{-1}\ cm^{-1}$ for the apoenzyme dimer and $\epsilon_{280} = 1.40\ 10^5\ M^{-1}\ cm^{-1}$ for the holoenzyme dimer. Enzyme activities were determined as previously described (Cournil et al., 1975) according to the method of Karmen (1955). The remaining activity of the apoenzyme was found to be less than 4% of the holoenzyme activity in all experiments, and the enzyme recovered full activity after addition of PLP. After preparation, the apoenzyme was used within 24 h.

Chemicals. Pyridoxal 5′-phosphate (PLP) ($\epsilon_{388} = 6.2\ 10^3\ M^{-1}\ cm^{-1}$ in 0.1 N NaOH) of the highest purity available, L-cysteinesulfinic acid, and NADH were purchased from

† From the Laboratoire d'Enzymologie Physico-chimique et moléculaire, Groupe de Recherche No. 13 du C.N.R.S., Batiment 433, Université de Paris-Sud, Centre d'Orsay 91405, France. *Received July 18, 1980.* This work was supported by grants from the Centre National de la Recherche Scientifique. This and previously published work (Vergé et al., 1979) has been carried out as a partial fulfillment of a doctoral thesis to be submitted by D.V.

[1] Abbreviations used: aspartate aminotransferase, L-aspartate:2-oxoglutarate aminotransferase (EC 2.6.1.1); PLP or pyridoxal-P, pyridoxal 5′-phosphate; TEA, triethanolamine.

0006-2960/81/0420-1210$01.25/0

Sigma. The purity of PLP was checked by its UV absorption spectrum in 0.1 N NaOH. Substrates 2-oxoglutaric acid and L-aspartic acid were from Calbiochem. Malate dehydrogenase was obtained from Boehringer. Triethanolamine (TEA) was from Merck.

Methods

Titration of apoenzyme was performed by adding aliquots of PLP to a solution of apoenzyme in 0.05 M TEA–HCl buffer, pH 8.3. Enzyme activity was measured, and the absorption spectrum was recorded with a Cary 16 K spectrophotometer; in some experiments only absorbance at 362 nm, instead of the absorption spectrum, was checked.

Stopped-flow measurements were carried out with a single-beam absorbance stopped-flow apparatus, Durrum Gibson Model 13002, as previously described (Kellershohn & Seydoux, 1979). The optical path length of the observation chamber was 1.75 cm. All experiments were carried out in 0.05 M TEA–HCl, pH 8.3, at 25 °C.

Data Acquisition. Two different systems of data acquisition were used. The first one was previously described (Kellershohn & Seydoux, 1979). The second one was designed and realized in our laboratory by M. Jousset; kinetic data were stored directly, during the experiment, into the memory of a Wang 2200B calculator; two time bases were available for the first 1024 points (from 0.5 to 50 ms per point), and further recording was possible with any desired time base constant larger than 50 ms (up to 5000 points). Slow processes could therefore be recorded. Further averaging, storage on magnetic tapes, and graphical plot of the kinetic data were possible.

Numerical Treatment of Kinetic Data. Analyses of the kinetic data (determination of the relaxation times and amplitudes) were performed according to general methods of multilinear regression with a Wang 2200 B calculator (BASIC programs from Dr. N. Kellershohn). The simulation studies of transient kinetic experiments were carried out by numerical integration of the appropriate set of differential equations [method of Kübicek & Visnak (1974); BASIC programs adapted from Dr. F. Seydoux]. The point-by-point construction of the successive absorption spectra during the reaction process from stopped-flow traces was performed with the same Wang 2200 B minicomputer.

Results

Titration of apoenzyme with PLP, by spectrophotometric and activity measurements, showed, as expected from literature data (Snell, 1970; Evangelopoulos & Sizer, 1965; Martinez-Carrion et al., 1970), that the equilibrium strongly favored the formation of holoenzyme, so that no equilibrium constant could be determined. The stoichiometry was found to be one molecule of PLP for one molecule of monomer. Actual concentrations of sites which can be reactivated were determined from these titrations and used in stopped-flow experiments.

Absorbance Change Associated with the Reconstitution Reaction at 362 nm When the PLP Concentration Is Considerably Higher Than the Apoenzyme Concentration. When the apoenzyme (2–5 μM) is mixed in the stopped-flow apparatus with a large excess of PLP (40–220 μM), the coenzyme binding monitored at 362 nm appears typically as in Figure 1. The 362-nm wavelength was chosen because it is the absorption maximum of bound coenzyme at pH 8.3 and also the wavelength at which the amplitude of the signal is a maximum ($\Delta\epsilon$ = 4500 M^{-1} cm^{-1}). The absorbance change obviously consists of two phases with opposite signs. The second phase was found to be itself composed of two distinct processes. The third phase could not be detected when the

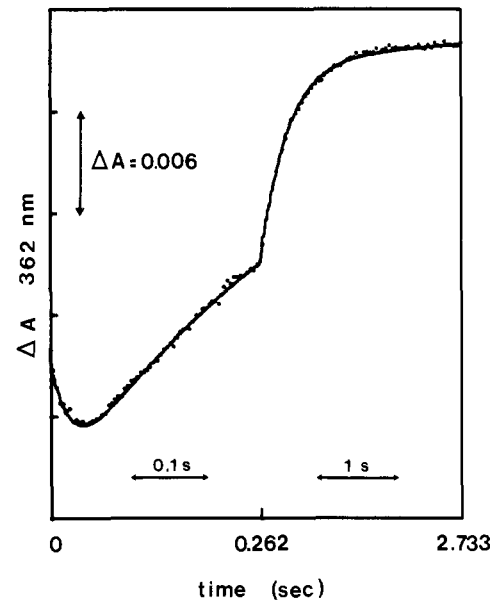

FIGURE 1: Kinetic trace of the absorbance change at 362 nm after rapid mixing of apoenzyme and pyridoxal-P in 0.05 M TEA-HCl buffer, pH 8.3. The final concentrations were $(apoAAT)_0$ = 4.3 μM, $(PLP)_0$ = 100 μM. Note the dual time base. The change of time base occurs at 262 ms. The fitted curve was calculated by numerical integration according to Scheme III with the kinetic parameters from Table I and the extinction coefficients $\epsilon(E_1)$ = 1500 M^{-1} cm^{-1}, $\epsilon(E_2)$ = 7600 M^{-1} cm^{-1}, $\epsilon(E_3)$ = 8200 M^{-1} cm^{-1}, ϵ(PLP) = 3700 M^{-1} cm^{-1}, ϵ(apoAAT) = 0.

PLP concentration was greater than 100 μM because of the slow reaction between PLP and the accessible lysines of the protein; the amplitude of this reaction became important and masked the end of the reconstitution reaction. Nevertheless, the reaction could be considered as the sum of three exponential processes.

Relaxation Time Analysis. We studied the dependence of the three relaxation times with respect to PLP concentration (Figure 2). The simplest mechanism consistent with the data is given by Scheme I, where A represents the apoenzyme, E_1 and E_2 represent the intermediate species, and E_3 represents the holoenzyme.

Scheme I

$$A + PLP \underset{k_{-1}}{\overset{k_1}{\rightleftharpoons}} E_1 \underset{k_{-2}}{\overset{k_2}{\rightleftharpoons}} E_2 \underset{k_{-3}}{\overset{k_3}{\rightleftharpoons}} E_3$$

One irreversible step is necessary to account for the irreversibility of the overall reaction. The observed independence of τ_3 with the PLP concentration is a good indication that the second step is irreversible. Let us consider now Scheme II.

Scheme II

$$A + PLP \underset{k_{-1}}{\overset{k_1}{\rightleftharpoons}} E_1 \overset{k_2}{\longrightarrow} E_2 \underset{k_{-3}}{\overset{k_3}{\rightleftharpoons}} E_3$$

We are in the conditions in which the differential equations derived from Scheme II can be linearized and solved (cf. Appendix). The secular equation is

$$[P_2 + P(k_1y_0 + k_{-1} + k_2) + k_1y_0k_2](P + k_3 + k_{-3}) = 0 \quad (1)$$

and from this equation we can deduce three relationships between the relaxation times and the individual rate constants:

$$k_1y_0 + k_{-1} + k_2 = 1/\tau_1 + 1/\tau_2 \quad (2)$$

$$k_1k_2y_0 = 1/\tau_1\tau_2 \quad (3)$$

$$k_3 + k_{-3} = 1/\tau_3 \quad (4)$$

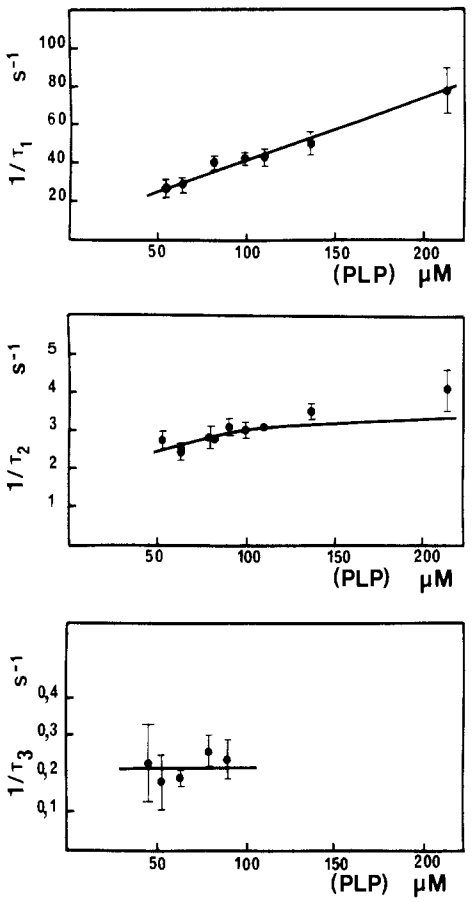

FIGURE 2: Dependence of the relaxation times on PLP concentration. The apoenzyme concentration was in the range 2.4–4.3 μM. The solid curves were calculated according to eq 1, with the kinetic parameters from Table I. Conditions were identical with those for Figure 1.

From the plots of $1/\tau_1 + 1/\tau_2$ and $1/\tau_1\tau_2$ vs. the concentration of PLP (Figure 3), we can determine two slopes and one intercept, and from these constants the values of k_1, k_{-1}, and k_2. A relationship is lacking to determine k_3 and k_{-3}. But we note that if k_3 and k_{-3} were of the same order of magnitude, two distinct forms of holoenzyme would be in slow equilibrium, which was never proved. So we shall assume $k_3 \gg k_{-3}$ and suppose that the third step is irreversible, consistent with Scheme III. The numerical values of the rate constants and

Scheme III

$$A + PLP \underset{k_{-1}}{\overset{k_1}{\rightleftharpoons}} E_1 \xrightarrow{k_2} E_2 \xrightarrow{k_3} E_3$$

the equilibrium constant for the first step of this scheme are given in Table I.

Amplitude Analysis. Scheme III is not the only scheme consistent with the experimentally determined relaxation times. Let us consider, for example, Schemes IV and V.

Scheme IV

$$A + PLP \xrightarrow{k_1} E_1 \xrightarrow{k_2} E_2$$

$$A \underset{k'_{-1}}{\overset{k'_1}{\rightleftharpoons}} A'$$

Scheme V

$$A' \underset{k'_1}{\overset{k'_{-1}}{\rightleftharpoons}} A + PLP \xrightarrow{k_1} E_1 \xrightarrow{k_2} E_2$$

The first mechanism (Scheme IV) postulates the existence of two distinct forms of apoenzyme in equilibrium, one of them being unable to bind PLP; and the second mechanism (Scheme V) accounts for the formation of an abortive complex. Both mechanisms can be solved by the general method used above. The secular equations are

$$(P + k_2)[P^2 + P(k'_1 + k'_{-1} + k_1y_0) + k'_{-1}k_1y_0] = 0 \quad (5)$$

for the Scheme IV and

$$(P + k_2)[P^2 + P[(k_1 + k'_1)y_0 + k'_{-1}] + k_1y_0k'_{-1}] = 0 \quad (6)$$

for Scheme V. Table II gives the individual rate constants and the equilibrium constants deduced from these equations. From the relaxation times analysis, we cannot, therefore,

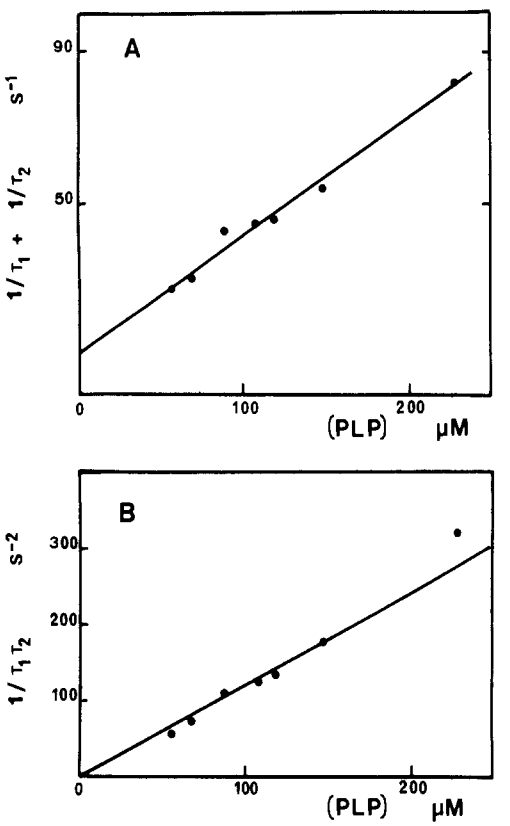

FIGURE 3: Plots of $1/\tau_1 + 1/\tau_2$ (A) and $1/\tau_1\tau_2$ (B) vs. pyridoxal-P concentration.

Table I: Rate and Equilibrium Constants[a]

i[b]	k_i	k_{-i}	K_i
1	0.32 10^6 M^{-1} s^{-1}	8.4 s^{-1}	2.63 10^{-5} M
2	3.9 s^{-1}		
3	0.22 s^{-1}		

[a] Determined for Scheme III from plots of the data according to eq 2–4. [b] For each step i (1, 2, or 3), k_i is the forward rate constant, k_{-i} the reverse rate constant, and K_i the equilibrium constant.

Table II: Rate and Equilibrium Constants[a]

scheme	i[b]	k_i	k_{-i}	K_i
IV	1	0.32 10^6 M^{-1} s^{-1}		
	2	0.22 s^{-1}		
	1′	8.4 s^{-1}	3.9 s^{-1}	0.46
V	1	0.11 10^6 M^{-1} s^{-1}		
	2	0.22 s^{-1}		
	1′	0.21 10^6 M^{-1} s^{-1}	12.3 s^{-1}	5.9 10^{-5} M

[a] Determined for Schemes IV and V from plots of the data according to eq 5-6. [b] See Table I.

Table III

scheme	i	phase amplitudes (A_i)
III[a]	1	$\frac{k_1x_0y_0}{\gamma_2-\gamma_1}\left(\Delta\epsilon_1+\frac{k_2}{k_3-\gamma_1}\Delta\epsilon_2-\frac{k_2k_3}{\gamma_1(k_3-\gamma_1)}\Delta\epsilon_3\right)$
	2	$\frac{k_1x_0y_0}{\gamma_1-\gamma_2}\left(\Delta\epsilon_1+\frac{k_2}{k_3-\gamma_2}\Delta\epsilon_2-\frac{k_2k_3}{\gamma_2(k_3-\gamma_2)}\Delta\epsilon_3\right)$
	3	$\frac{k_1x_0y_0k_2}{(\gamma_1-k_3)(\gamma_2-k_3)}(\Delta\epsilon_2-\Delta\epsilon_3)$
IV[b]	1	$\frac{k_1y_0x_0(k'_1+k'_{-1}-\gamma_1)}{(\gamma_2-\gamma_1)(k_2-\gamma_1)}\left(\Delta\epsilon_1-\frac{k_2}{\gamma_1}\Delta\epsilon_2\right)$
	2	$\frac{k_1x_0y_0(k'_1+k'_{-1}-\gamma_2)}{(\gamma_1-\gamma_2)(k_2-\gamma_2)}\left(\Delta\epsilon_1-\frac{k_2}{\gamma_2}\Delta\epsilon_2\right)$
	3	$\frac{k_1x_0y_0(k'_1+k'_{-1}-k_2)}{(\gamma_1-k_2)(\gamma_2-k_2)}(\Delta\epsilon_1-\Delta\epsilon_2)$
V[c]	1	$\frac{x_0y_0}{\gamma_2-\gamma_1}\left[k'_1\Delta\epsilon'+\frac{(k'_{-1}-\gamma_1)k_1}{k_2-\gamma_1}\left(\Delta\epsilon_1-\frac{k_2}{\gamma_1}\Delta\epsilon_2\right)\right]$
	2	$\frac{x_0y_0}{\gamma_1-\gamma_2}\left[k'_1\Delta\epsilon'+\frac{(k'_{-1}-\gamma_2)k_1}{k_2-\gamma_2}\left(\Delta\epsilon_1-\frac{k_2}{\gamma_2}\Delta\epsilon_2\right)\right]$
	3	$\frac{k_1y_0x_0(k'_{-1}-k_2)}{(\gamma_1-k_2)(\gamma_2-k_2)}(\Delta\epsilon_1-\Delta\epsilon_2)$

[a] $-\gamma_1$ and $-\gamma_2$ are roots of eq 1, with $\gamma_1>\gamma_2$. $\Delta\epsilon_3=4500$ M^{-1} cm^{-1}. [b] $-\gamma_1$ and $-\gamma_2$ are roots of eq 5, with $\gamma_1>\gamma_2$. $\Delta\epsilon_2=4500$ M^{-1} cm^{-1}. $x_0=E_t/(1+1/K)$, $K=k'_{-1}/k'_1$. [c] $-\gamma_1$ and $-\gamma_2$ are roots of eq 6, with $\gamma_1>\gamma_2$. $\Delta\epsilon_3=4500$ M^{-1} cm^{-1}.

decide which of the mechanisms applies.

This ambiguity can be removed by a detailed analysis of the amplitudes of the exponential processes. The amplitudes of the three phases were found to be almost constant in the range of concentrations used, with $A_1 = 2100 \pm 300$ M^{-1} cm^{-1}, $A_2 = -6000 \pm 500$ M^{-1} cm^{-1}, and $A_3 = -600 \pm 100$ M^{-1} cm^{-1}. By a method similar to that described in the Appendix for Scheme II, we derived the absorbance time course corresponding to each mechanism; the phase amplitudes are detailed in Table III. We can first observe that the extinction coefficient of E_3 (Scheme III) or E_2 (Schemes IV and V) is always 8200 M^{-1} cm^{-1}, since this species is holoenzyme. Furthermore, all models predict that the extinction coefficient of the last intermediate is 7600 M^{-1} cm^{-1}. Scheme IV can be immediately discarded because the calculated amplitudes A_1 and A_2 with $\epsilon_1 = 7600$ M^{-1} cm^{-1} and $\epsilon_2 = 8200$ M^{-1} cm^{-1} ($A_1 = -700$ M^{-1} cm^{-1} and $A_2 = -3100$ M^{-1} cm^{-1}) do not agree with the experimental data. For Schemes III and V, the only unknown parameter is the extinction coefficient of the first intermediate E_1 (Scheme III) or A′ (Scheme V). In the case of Scheme V, we could not find a value of this extinction coefficient satisfying simultaneously the equations $A_1 = 2100$ and $A_2 = -6000$. On the contrary, these equations were satisfied in the case of Scheme III, with $\epsilon_1 = 1500$ M^{-1} cm^{-1}. The mechanism postulated in Scheme III is therefore consistent with both relaxation time and amplitude data when the following extinction coefficients are assigned to the intermediate species:

$$\epsilon_1 = 1500 \text{ M}^{-1} \text{ cm}^{-1}$$

$$\epsilon_2 = 7600 \text{ M}^{-1} \text{ cm}^{-1}$$

The simulation studies of the reaction gave quite good fittings of the data (Figure 1). We tried to see if other simple schemes could be consistent with the data. It was not the case for branched schemes such as Scheme VI. The secular equation for this mechanism is given by eq 7.

Scheme VI

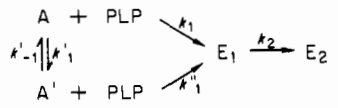

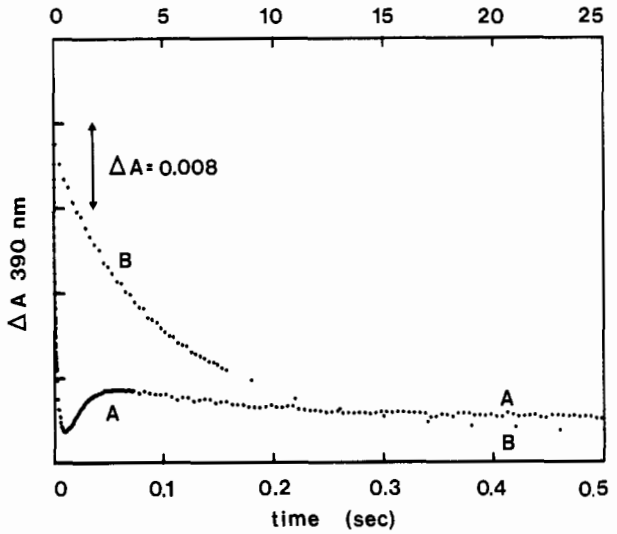

FIGURE 4: Kinetic trace of the absorbance change at 390 nm after rapid mixing of apoenzyme and pyridoxal-P in stoichiometric conditions. The final concentrations were $(apoAAT)_0 = 9$ μM, $(PLP)_0 = 9$ μM. Curve A, overall kinetics (upper time scale); curve B, expanded trace of the beginning of the process (lower time scale).

$$(P + k_2)[P^2 + P(y_0k_1 + y_0k''_1 + k'_1 + k'_{-1}) + k_1k''_1y_0^2 + y_0(k_1k'_{-1} + k''_1k'_1)] = 0 \quad (7)$$

So we should have

$$1/\tau_1\tau_2 = k_1k''_1y_0^2 + y_0(k_1k'_1 + k''_1k'_1) \quad (8)$$

and then observe a nonlinear variation of $1/\tau_1\tau_2$ as a function of y_0, which is not the case.

Stopped-Flow Studies under Stoichiometric Conditions. For determination of the spectra of the intermediates during the reconstitution of holoaspartate aminotransferase, the reaction between apoenzyme and PLP was studied at various wavelengths (in the range 340–450 nm) under stoichiometric conditions. Direct evidence of the occurrence of at least three phases in the process is given by kinetics observed at 390 nm (Figure 4): at this wavelength, the absorbance successively decreases, then increases, and finally decreases. Unfortunately, simulations of the experiments performed under stoichiometric conditions on the basis of Scheme III were not satisfactory. Thus, Scheme III is insufficient and the actual mechanism is probably more complex. However, we were able to reconstitute point by point the variation of the absorption spectrum during the reaction course (Figure 5). An isosbestic point is observed around 385 nm for the end of the reaction. It is likely that it is the isosbestic point for the isomerization of the last intermediate species (giving the holoenzyme).

It is difficult to gain information about the fast intermediate species because, as can be seen from Figure 6, in the hypothesis of Scheme III, this species never accounts for more than 15% of the total enzyme. On the contrary, the end of the reaction can be analyzed separately. The process follows first-order kinetics, with a mean rate constant 0.12 s^{-1}, close to the one found for the last phase in Scheme III. This result is consistent with the hypothesis of a slow step decoupled from the others. In spite of the small amplitude of this phase, a spectrum of

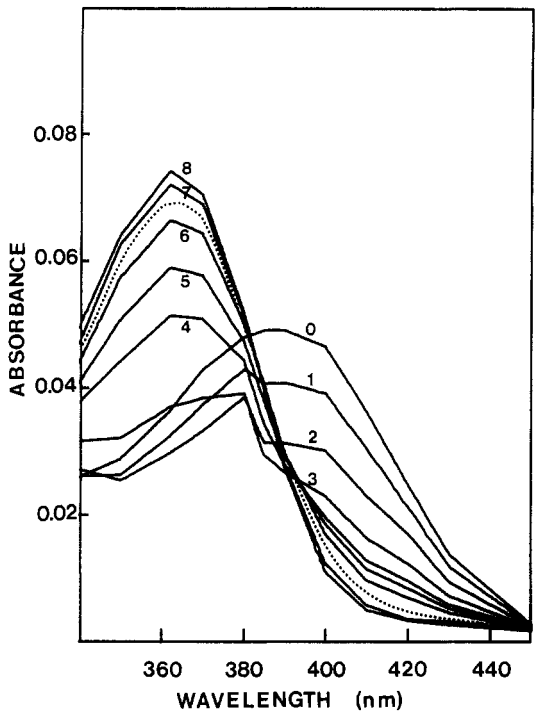

FIGURE 5: Variation of the absorption spectrum during the reaction of apoenzyme (final concentration 9 μM) and pyridoxal-P (final concentration 9 μM), as reconstituted point by point from stopped-flow experiments. Curve 0, t = 0; curve 1, t = 38 ms; curve 2, t = 158 ms; curve 3, t = 500 ms; curve 4, t = 1.14 s; curve 5, t = 1.74 s; curve 6, t = 3.34 s; curve 7, t = 21.34 s; curve 8, t = ∞; dashed curve, reconstituted spectrum of the last intermediate.

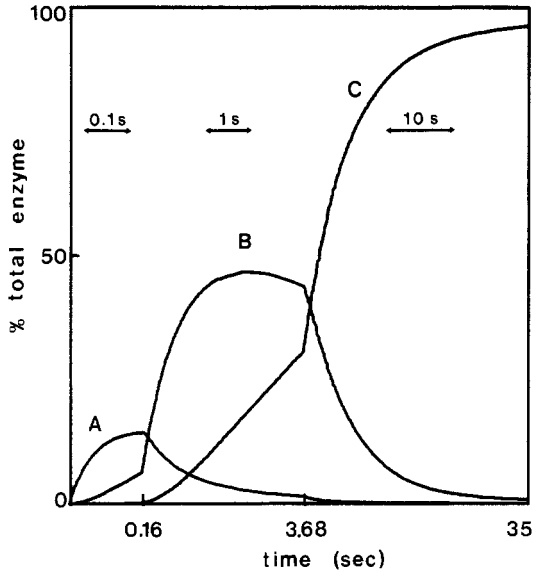

FIGURE 6: Simulation of the reconstitution reaction under stoichiometric conditions. Variation of the concentrations of the intermediate species with respect to time. Calculations were made as in Figure 1, with $(\text{apoAAT})_0 = (\text{PLP})_0 = 9$ μM. Curve A, first species, E_1; curve B, second species, E_2; curve C, last species, E_3, holoenzyme. Other species (apoenzyme and pyridoxal-P) were omitted for clarity. Note the two changes of time base, at 0.16 s and 3.68 s.

the last intermediate (E_2) was tentatively drawn (Figure 5). This spectrum is very similar to the holoenzyme spectrum, with a maximum at 365 nm and a slightly larger bandwidth.

Discussion

The mechanism of the reconstitution reaction of holoaspartate aminotransferase from apoenzyme and pyridoxal 5′-phosphate appears highly complex. This fact is not surprising since previous studies carried out under various conditions showed that the reaction proceeded through at least two steps (Banks et al., 1963; Churchich & Farrelly, 1968; Bocharov et al., 1968; Fonda & Auerbach, 1976) or four steps (Arrio-Dupont, 1969). It is known that the reconstitution behavior of the apoenzyme is very dependent on the method of resolution (Arrio-Dupont, 1972). The presence of inorganic phosphate, which binds tightly to the apoenzyme, probably to the same binding site as PLP (Vergé et al., 1979), is critical during the procedure of resolution. It is probably the reason why Fonda & Auerbach (1976), when studying the reconstitution kinetics with an apoenzyme prepared according to Furbish et al. (1969), found an overall rate lower than the one which we observe. Arrio-Dupont (1972) showed that their apoenzyme contained two phosphate ions tightly bound, which probably act as inhibitors of the reaction of reconstitution since PLP must displace them.

The analysis of our kinetics, obtained with an apoenzyme free of inorganic phosphate, shows that the process involves at least three steps. This fact is proved (a) by the analysis of the experiments performed in an excess of PLP at 362 nm—the signal is the sum of at least three exponential processes—and (b) by the absorbance change observed in stoichiometric conditions at 390 nm. The occurrence of three steps in such a reaction is a common feature; it was shown for the binding of PLP to apoglutamate decarboxylase (O'Leary & Malik, 1972) and D-serine apodehydratase (Reed & Schnackerz, 1979). However, in these two cases, no direct evidence for three distinct steps was presented.

The detailed analysis of the stopped-flow experiments when PLP was in excess allowed us to propose a mechanism (Scheme III) in which the initial reversible binding of PLP was followed by two irreversible steps. It must be pointed out that the last step has a low amplitude ($\Delta\epsilon$ = 600 M^{-1} cm^{-1}) and that the independence of the corresponding relaxation time with PLP concentration is not very obvious, because of the lack of data at high concentrations. Nevertheless, the detection of this slow decoupled step in stoichiometric conditions is good evidence that it actually occurs. The mechanism described in Scheme III was the "minimal" scheme we found to be consistent with the data obtained in the presence of an excess of PLP.

The study of the reconstitution under the stoichiometric conditions strongly suggests that the mechanism is more complex, since a good fit of the data could not be done with Scheme III. Besides the possibility of additional steps, or branching in the mechanism, we cannot exclude an effect of the equilibrium between PLP, water, and the hydrate of PLP. At pH 8.3, the percentage of PLP in the hydrated form is around 10% (Morozov et al., 1967), and the rate constants of the hydration reaction are of the same order of magnitude as the rate constants of the reconstitution (Reed & Schnackerz, 1979). The hydrate of PLP cannot form the Schiff base, and the equilibrium $H_2O + \text{PLP} \rightleftharpoons \text{PLP}_h$ is therefore displaced toward the dissociation during the course of the reconstitution reaction. This effect can be neglected when PLP is in excess, but probably not in the stoichiometric conditions.

Another explanation for the inadequacy of the proposed mechanism is the occurrence of interactions between the subunits of the dimer. Recent evidence in favor of such interactions has been presented: e.g., inactivity of the monomer (Arrio-Dupont & Coulet, 1979) and proximity of the two active sites in the dimer demonstrated by X-ray diffraction studies (Borisov et al., 1978, Eichele et al., 1979). Therefore, a mechanism similar to the one already proposed by Arrio-Dupont (1969) is suggested in Scheme VII.

Scheme VII

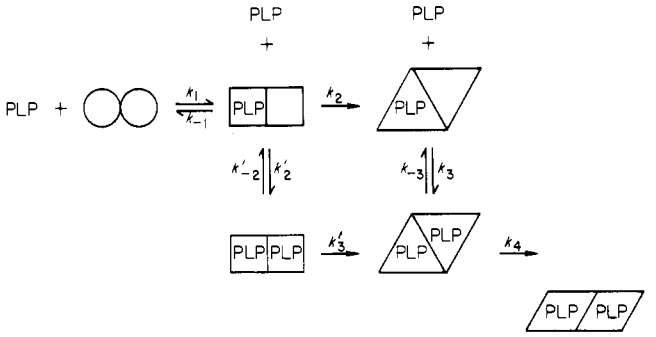

Under conditions of excess of PLP, if k'_2 (PLP) $\gg k_2$, the pathway is the same as in Scheme III, but under stoichiometric conditions, the alternative pathway, in which the conformational change occurs before the binding of the second molecule of PLP may interfere with the major pathway described in Scheme III. It is also possible that the two phenomena arise simultaneously. An effect of the dissociation of the dimer into monomers can be ruled out since in the concentration range used (2–5 μM) it has been shown that the proportion of monomers is negligible (Cournil et al., 1975).

From the calculated rate constants we can deduce the equilibrium constant for the first step of Scheme III, K_D = 2.6 10^{-5} M. This value is in good agreement with the results of Fonda & Auerbach (1976), who found $K_D = 10^{-5}$ M for the first step of the process. The spectrum attributed to the last intermediate, E_2, indicates that only a small conformational change occurs during the last step, since this spectrum is close to that of the holoenzyme. These facts can be compared with the results of Churchich & Farrelly (1968), who observed that in the presence of inorganic phosphate Schiff base formation was fast whereas the recovery of catalytic activity was very slow. They concluded that an inactive Schiff base was an intermediate in the process and that the activity appeared during a conformational change following the formation of the covalent bond. So we can consider two possible interpretations of Scheme III: (a) reversible formation of the Schiff base during the first step, followed by two steps of isomerization. (b) An adsorption binding step (1), formation of the covalent bond (2), and an isomerization step (3). In the second case, the mechanism would be very similar to the one proposed by Reed & Schnakerz (1979) for binding of PLP to D-serine apodehydratase.

It is likely that conformational changes occur in the protein at least during the isomerization steps. A direct study of these structural changes of the protein moiety, as reflected by the fluorescence of tryptophan residues, is proceeding in our laboratory.

Acknowledgments

We thank Dr. J. Yon, Director of Groupe de Recherches No. 13, for her interest in this work, J. Carrette for excellent technical assistance, and Professor P. Shannon for careful reading of the manuscript.

Appendix

For Scheme II, if we assume that the PLP concentration remains constant, the set of differential equations is

$$\dot{x} = -k_1 x y_0 + k_{-1} x_1$$
$$\dot{x}_1 = k_1 x y_0 - (k_{-1} + k_2) x_1$$
$$\dot{x}_2 = k_2 x_1 + k_{-3} x_3 - k_3 x_2$$
$$\dot{x}_3 = k_3 x_2 - k_{-3} x_3$$

where x represents the apoenzyme concentration, y_0 is the PLP concentration, and x_1, x_2, and x_3 are the concentrations of the intermediate species. $\dot{x}$, $\dot{x}_1$, $\dot{x}_2$, $\dot{x}_3$ are the derivatives of x, x_1, x_2, x_3, with respect to time. This system can be solved easily by means of the Laplace–Carson transform (Rodiguin & Rodiguina, 1964). The relaxation times are found to be roots of the secular determinant.

$$|B| = \begin{vmatrix} k_1 y_0 + P & -k_{-1} & 0 & 0 \\ -k_1 y_0 & k_{-1} + k_2 + P & 0 & 0 \\ 0 & -k_2 & k_3 + P & -k_{-3} \\ 0 & 0 & -k_3 & k_{-3} + P \end{vmatrix} = 0 \quad \text{(A1)}$$

This equation has one root equal to zero (the four equations are nonindependent) and three negative roots ($P_i = -1/\tau_i$). After solvation, one can show that

$$x_i(t) = a_{i0} + \sum_{j=1}^{3} a_{ij} e^{P_j t} \quad \text{(A2)}$$

where the a_{ij} are functions of the individual rate constants and the relaxation times. Let ϵ_0 be the extinction coefficient of PLP, ϵ the extinction coefficient of the apoenzyme (assumed to be 0), and ϵ_i the extinction coefficient of the E_i species. The instantaneous absorbance is

$$A(t) = \epsilon_0 y + \sum_{i=1}^{3} \epsilon_i x_i(t) \quad \text{(A3)}$$

The conservation equation for PLP is

$$y_0 - y = \sum_{i=1}^{3} x_i \quad \text{(A4)}$$

So we can write

$$A(t) = \epsilon_0 y_0 + \sum_{i=1}^{3} (\epsilon_i - \epsilon_0) x_i(t) \quad \text{(A5)}$$

or with $\epsilon_i - \epsilon_0 = \Delta\epsilon_i$

$$A(t) = \epsilon_0 y_0 + \sum_{i=1}^{3} \Delta\epsilon_i x_i(t) \quad \text{(A6)}$$

or

$$A(t) = \epsilon_0 y_0 + \sum_{i=1}^{3} \Delta\epsilon_i a_{i0} + \sum_{i=1}^{3}\sum_{j=1}^{3} \Delta\epsilon_i a_{ij} e^{P_j t} \quad \text{(A7)}$$

At the end of the reaction, we have

$$A(\infty) = \epsilon_0 y_0 + \sum_{i=1}^{3} \Delta\epsilon_i a_{i0} \quad \text{(A8)}$$

Therefore

$$A(t) - A(\infty) = \sum_{j=1}^{3} \left(\sum_{i=1}^{3} \Delta\epsilon_i a_{ij}\right) e^{P_j t} \quad \text{(A9)}$$

The amplitude of each phase can therefore be calculated.

$$A_j = \sum_{i=1}^{3} \Delta\epsilon_i a_{ij} \quad \text{(A10)}$$

References

Abaturov, L. V., Polyanovsky, O. L., Torchinsky, Yu. M., & Varshavsky, Ya. M. (1968) in *Pyridoxal Catalysis: Enzymes and Model Systems* (Snell, E. E., Braunstein, A. E., Severin, E. S., & Torchinsky, Yu. M., Eds.) pp 171–177, Wiley, New York.

Arrio-Dupont, M. (1969) *Biochem. Biophys. Res. Commun. 36*, 306–311.

Arrio-Dupont, M. (1972) *Eur. J. Biochem. 30*, 307–317.

Arrio-Dupont, M. (1978) *Eur. J. Biochem. 91*, 369–378.
Arrio-Dupont, M., & Coulet, P. R. (1979) *Biochem. Biophys. Res. Commun. 89*, 345–352.
Banks, B. E. C., Lawrence, A. J., Vernon, C. A., & Wootton, J. F. (1963) in *Chemical and Biological Aspects of Pyridoxal Catalysis* (Snell, E. E., Fasella, P. M., Braunstein, A., & Rossi Fanelli, A., Eds.) pp 197–215, Pergamon Press, Oxford.
Bocharov, A. L., Ivanov, V. I., Karpeisky, M. Ya., Mamaeva, O. K., & Florentiev, V. L. (1968) *Biochem. Biophys. Res. Commun. 30*, 459–464.
Borisov, V. V., Borisova, S. N., Kachalova, G. S., Sosfenov, N. I., Voronova, A. A., Vainshtein, B. K., Torchinsky, Yu. M., & Braunstein, A. E. (1978) *J. Mol. Biol. 125*, 275–292.
Braunstein, A. E. (1973) *Enzymes, 3rd Ed. 9*, 379–481.
Churchich, J. E., & Farrelly, J. G. (1968) *Biochem. Biophys. Res. Commun. 31*, 316–321.
Cournil, I., Barba, J. M., Vergé, D., & Arrio-Dupont, M. (1975) *J. Biol. Chem. 250*, 8564–8568.
Eichele, G., Ford, G. C., Glor, R., Jansonius, J. N., Mavrides, C., & Christen, P. (1979) *J. Mol. Biol. 133*, 161–180.
Evangelopoulos, A. E., & Sizer, I. W. (1965) *J. Biol. Chem. 240*, 2983–2993.
Fonda, M. L., & Auerbach, S. B. (1976) *Biochim. Biophys. Acta 422*, 38–47.
Furbish, F. S., Fonda, M. L., & Metzler, D. E. (1969) *Biochemistry 8*, 5169–5180.
Ivanov, V. I., Bocharov, A. L., Volkenstein, M. V., Karpeisky, M. Ya., Mora, S., Okina, E. I., & Yudina, L. V. (1973) *Eur. J. Biochem. 40*, 519–526.
Karmen, A. (1955) *J. Clin. Invest. 34*, 131–133.
Kellershohn, N., & Seydoux, F. J. (1979) *Biochemistry 18*, 2465–2470.
Kübicek, M., & Visnak, K. (1974) *Chem. Eng. Commun. 1*, 291–296.
Martinez-Carrion, M., Turano, C., Chiancone, E., Bossa, F., Giartosio, A., Riva, F., & Fasella, P. (1967) *J. Biol. Chem. 242*, 2397–2409.
Martinez-Carrion, M., Kuczenski, R., Tiemeier, D. C., & Peterson, D. L. (1970) *J. Biol. Chem. 245*, 799–805.
Morozov, Yu. V., Bazhulina, N. P., Cherkashina, L. P., & Karpeisky, M. Ya. (1967) *Biofizika 12*, 397–406.
O'Leary, M. H., & Malik, J. M. (1972) *J. Biol. Chem. 247*, 7097–7105.
Reed, T. A., & Schnackerz, K. D. (1979) *Eur. J. Biochem. 94*, 207–214.
Rodiguin, N. M., & Rodiguina, E. N. (1963) *Consecutive Chemical Reactions: Mathematical Analysis and Development* (Schneider, R. F., Ed.) D. Van Nostrand, Princeton, NJ.
Scardi, V., Scotto, P., Iaccarino, M., & Scarano, E. (1963) *Biochem. J. 88*, 172–175.
Snell, E. E. (1970) *Vitam. Horm. 28*, 265–290.
Vergé, D., Tenu, J.-P., & Arrio-Dupont, M. (1979) *FEBS Lett. 100*, 265–268.
Wada, H., & Snell, E. E. (1962) *J. Biol. Chem. 237*, 127–132.

Comparison of the Early Histone H4 Gene Sequence of *Strongylocentrotus purpuratus* with Maternal, Early, and Late Histone H4 mRNA Sequences†

Michael Grunstein,* Kathleen E. Diamond, Eva Knoppel, and Judith E. Grunstein

ABSTRACT: A shift occurs in the utilization of histone mRNAs during early embryogenesis of the sea urchin. Maternal histone mRNAs are present in the unfertilized egg and can be utilized during early embryogenesis until the blastula stage. Soon after fertilization of the egg, a family of several hundred (early) histone genes are activated. During blastulation the mRNA products of these genes gradually disappear from the polysomes and are replaced by a new class of (late) histone mRNAs that differ in size and sequence and code for a new group of histone proteins. A sequence comparison of these three classes of histone H4 mRNAs to the cloned early H4 gene sequence is described. Early H4 gene fragments were used as primers for dideoxynucleotide sequence analysis of maternal and early H4 mRNAs. Portions of both translated and untranslated regions were compared. It was shown that these segments, comprising 26% of maternal and early H4 mRNAs, have the same sequence. The same early H4 gene fragments did not serve as primers for dideoxynucleotide sequencing of late H4 mRNA under the conditions of hybridization. Therefore late H4 mRNAs would not have been detected in the egg even if they were present there. Early and late H4 mRNAs were labeled in vivo and analyzed by using ribonuclease T_1 and a two-dimensional "fingerprint" separation. These oligonucleotides were compared to the early H4 gene sequence. Divergence between early and late H4 mRNAs was shown to be extensive. Within a selected portion of the gene there is a minimum of 9.4% divergence. This divergence has affected both translated and untranslated regions. It is concluded that an early H4 mRNA sequence is synthesized prior to fertilization and is then stored in the egg. A similar if not identical sequence is synthesized after fertilization until the mesenchyme blastula stage. It is then replaced on polysomes by a highly divergent late H4 messenger RNA.

Histone genes of the sea urchin are repeated several hundred times per haploid genome (Kedes & Birnstiel, 1971; Weinberg et al., 1972; Grunstein et al., 1973a; Grunstein & Schedl, 1976). The basic repeat unit is a DNA sequence, approximately 6500 bases in length, which contains the genes for histones H1, H4, H2B, H3 and H2A, in that order (Schaffner et al., 1976; Wu et al., 1976; Cohn et al., 1976). These repeats are tandemly arranged in the genome in an undetermined number of clusters (Kedes & Birnstiel, 1971; Birnstiel et al., 1974). However, the histone gene family is

† From the Molecular Biology Institute and Department of Biology, University of California, Los Angeles, California 90024. *Received August 5, 1980.* This work was supported by grants from the National Institutes of Health and the National Foundation March of Dimes. M.G. is the recipient of a Faculty Research Award from the American Cancer Society. K.D. received an N.I.H. postdoctoral fellowship.

0006-2960/81/0420-1216$01.25/0